RSC Advances

PAPER

View Article Online
View Journal | View Issue

Cite this: *RSC Adv.*, 2021, **11**, 11004

Synthesis, characterization, and photoelectric properties of iridium(III) complexes containing an N hetero-dibenzofuran C^N ligand†

Zequn Ma,[a] Chaojun Jing,*[a] Deyu Hang,[b] Hongtao Fan,[b] Lumeng Duan,[b] Shuqing Fang[b] and Li Yan[a]

Received 17th December 2020
Accepted 26th February 2021

DOI: 10.1039/d0ra10584h

rsc.li/rsc-advances

In this study, three high-efficient green light iridium(III) complexes were designed and synthesized, wherein 2-methyl-8-(2-pyridine) benzofuran [2,3-*B*] pyridine (MPBFP) is the main ligand and three β-diketone derivatives, namely 3,7-diethyl-4,6-nondiazone (detd), 2,2,6,6-tetramethyl-3,5-heptyldione (tmd) and acetylacetone (acac), are ancillary ligands. The thermal stabilities, electrochemical properties, and electroluminescence (EL) performance of these three complexes, namely $(MPBFP)_2$ Ir(detd), $(MPBFP)_2$Ir(tmd) and $(MPBFP)_2$Ir(acac), were investigated. The results show that the absorption peaks of the three complexes range from 260 to 340 nm, and the maximum emission wavelengths are 537 nm, 544 nm and 540 nm, respectively. The LUMO level is −2.18 eV, −2.20 eV, −2.21 eV, and the HOMO level is −5.30 eV, −5.25 eV, and −5.25 eV, respectively. The thermal decomposition temperatures of each of the three compounds are 359 °C, 389 °C and 410 °C respectively, with a weight loss of 5%. Green phosphorescent electroluminescent devices were prepared with the structure of ITO/HAT-CN/TAPC/TCTA/TCTA:X/Bepp2/LiF/Al, and the three complexes were dispersed in the organic light-emitting layer as the guest material X. The maximum external quantum efficiency of the devices is 17.2%, 16.7%, and 16.5%, respectively. The maximum brightness is 57 328 cd m^{-2}, 69 267 cd m^{-2} and 69 267 cd m^{-2}, respectively. With respect to the EL properties, $(MPBFP)_2$Ir(detd) is the best performer among the three complexes. The different performances exhibited by these complexes were discussed from the view point of substituent effect on the β-diketone ligands.

1. Introduction

In recent years, organic light emitting diodes (OLEDs) have attracted considerable attention due to their wide applications in the field of electronics technology,[1–3] such as display devices and solid state lighting. However, several key issues of OLED panels such as cost, efficiency and lifetime still need to be optimized before wide market application, among which organic lighting materials is the most important one. Therefore, the development of high-efficient, low cost and long-lived luminescent materials is the focus of numerous studies. Green light is one of the three primary colors of display systems; therefore, the demand for high-performance green emitters is very urgent. In metallic iridium–ligand complexes, electron jumping energy between the ground state, singlet excited state and triplet excited state can be utilized simultaneously due to the heavy atom effects and strong spin orbit coupling effects, which improve the theoretical internal quantum efficiency from 25% to 100%.[4–14] Simultaneously, the iridium-containing metal complexes show strong phosphorescence emission, and their efficiency and emission properties can be modified by changing the main C^N ligands and auxiliary ligands.[15–17] Recently, Zeng *et al.* have designed and synthesized an efficient green-yellow light iridium complex based on phenyl benzimidazole as the cyclometalated ligand and pyridine triazole as the ancillary ligand.[18] With 5-methyl-2-phenylpyridine as the main ligand and 3,7-diethyl-4,6-nondiazone as the auxiliary ligand, Fang *et al.* have reported three green phosphorescent metal iridium complexes with high luminescence performance.[19]

In this study, we have designed and synthesized a new main ligand, namely 2-methyl-8-(-pyridyl) coumarone [2,3-*B*] pyridine (MPBFP), and then have prepared three new green light-emitting iridium complexes using MPBFP as C^N type ligand and three β-diketones, namely 3,7-diethyl-4,6-nondiazone (detd), 2,2,6,6-tetramethyl-3,5-heptyldione (tmd) and acetylacetone (acac), as auxiliary ligands. The obtained metal iridium complexes, namely $(MPBFP)_2$Ir(detd), $(MPBFP)_2$Ir(tmd) and $(MPBFP)_2$Ir(acac), were systematically characterized and the luminescence performance was studied.

[a]*School of Chemistry and Chemical Engineering, Beijing Institute of Technology, Beijing, 100081, P. R. China. E-mail: jingcj@bit.edu.cn*

[b]*Beijing Yanhua Jilian Optoelectronics Co., LTD, Beijing, 102488, P. R. China*

† Electronic supplementary information (ESI) available. CCDC 2024173. For ESI and crystallographic data in CIF or other electronic format see DOI: 10.1039/d0ra10584h

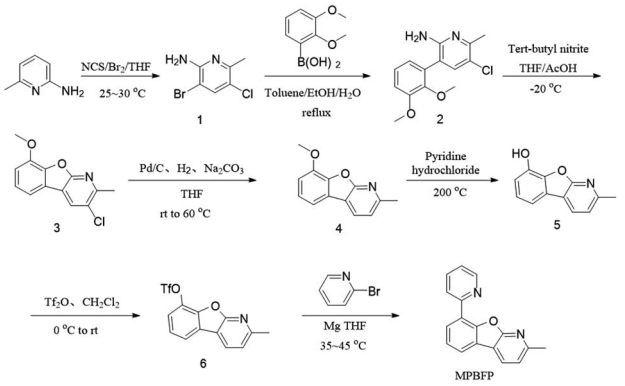

Scheme 1 Synthesis route of 1,2-methyl-8-(2-pyridine)benzofuran [2,3-*B*] pyridine (MPBFP).

2. Experimental procedure

2.1 Chemicals and materials

Iridium trichloride hydrate ($IrCl_3 \cdot H_2O$, Ir > 54% by weight) was purchased from Guiyan platinum Co., Ltd. Bromine, *tert*-butyl nitrite, trifluoromesylate and 2,3-dimethoxybenzene boric acid (AR), were purchased from Shanghai Macklin Bio-technology Co., Ltd. acac, tmd, and detd were purchased from Beijing Yanhua Lumen Technology Co., Ltd. Bis(triphenylphosphine) palladium chloride (palladium mass fraction 15%) was purchased from Beijing Zhongsheng Huateng technology Co., LTD. Ethylene glycol ether (AR) was purchased from Nanjing Opchi Pharmaceutical Co., LTD. *N*-Closuccinimide was purchased from Shanghai Kangkuo Chemical Co., LTD. 4-Triphenylphosphine palladium (AR) was purchased from Shanxi Ruike new materials Co., LTD. The regents were used as received unless otherwise stated.

2.2 Synthesis of the C^N ligand

Main ligand MPBFP was synthesized according to the method shown in Scheme 1.

2.3 Preparation of metal complexes

Three iridium(III) complexes were prepared according to the procedure displaced in Scheme 2, in which MPBFP is the main ligand and three diketone derivatives, namely detd, tmd and acac, are ancillary ligands.

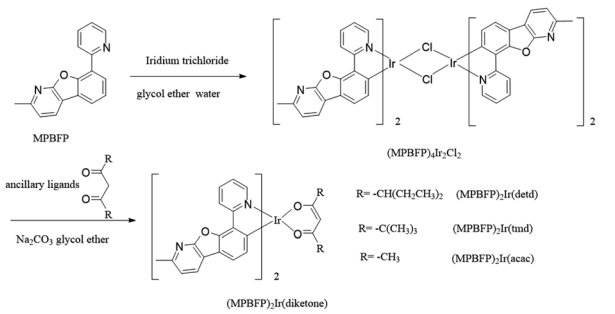

Scheme 2 Preparation of the chlorine-bridging dimer $(MPBFP)_4Ir_2Cl_2$ and three target metal complexes, namely $(MPBFP)_2Ir(detd)$, $(MPBFP)_2Ir(tmd)$ and $(MPBFP)_2Ir(acac)$.

3. Results and discussion

3.1 Thermo gravimetric analysis

In order to investigate the thermal stability of the three complexes, thermo gravimetric analysis (TGA) was conducted using a NETZSCH instruments TG 209 F3 Tarsus from 20 °C to 800 °C at a heating rate of 20 °C min^{-1} under nitrogen atmosphere, and the result is shown in Fig. 1.

The temperatures at which compounds $(MPBFP)_2Ir(detd)$, $(MPBFP)_2Ir(tmd)$ and $(MPBFP)_2Ir(acac)$ 5% weight loss are 359, 389 and 410 °C, respectively, indicating that the three complexes have high thermal stabilities (>350 °C), which is a very important requirement for the evaporation process in OLED device preparation. Among the three compounds, $(MPBFP)_2Ir(acac)$ displays the best thermal stability (410 °C), followed by $(MPBFP)_2Ir(tmd)$ (389 °C), and $(MPBFP)_2Ir(detd)$ exhibits the lowest stability (359 °C). This may be related to the substituent effects on the β-diketone ligands. For example, detd has two pentyl groups in the molecular structure, tmd has two *tert*-butyl groups in the molecular structure, and acac has two methyl groups on the diketone's backbone. Pentyl groups in detd are long and soft hydrocarbon chains, which are good for solubility and easy to degrade under high temperature *via* C–H bond homolysis. *Tert*-butyl and methyl groups are much smaller and rigid; therefore, $(MPBFP)_2Ir(tmd)$ and $(MPBFP)_2Ir(acac)$ showed better thermal stability.

3.2 Single crystal structure

Single crystals of iridium complex $(MPBFP)_2Ir(detd)$ were prepared by the co-volatilization of a mixture of dichloromethane and heptane. The $(MPBFP)_2Ir(detd)$ crystal information was obtained on a Bruker APEXII DUO X-ray single crystal diffractometer and the single crystal structure, ellipsoid (hydrogen atoms omitted), is shown in Fig. 2.

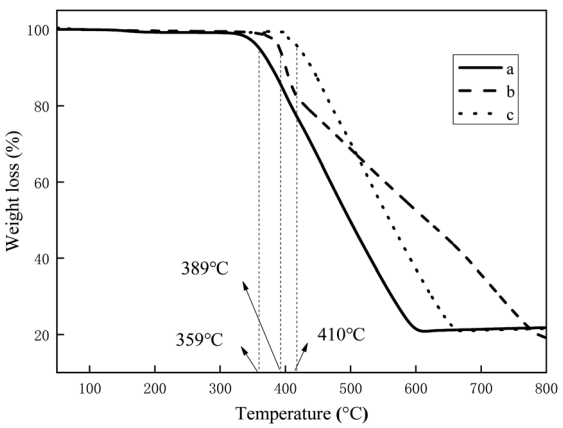

Fig. 1 The TGA curves of the three complexes: (a) $(MPBFP)_2Ir(detd)$, (b) $(MPBFP)_2Ir(tmd)$, and (c) $(MPBFP)_2Ir(acac)$.

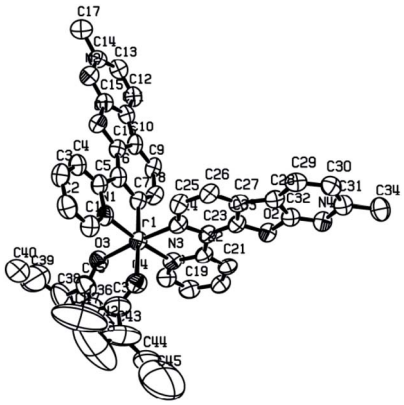

Fig. 2 $(MPBFP)_2Ir(detd)$ single crystal structure ellipsoid, CCDC deposition number: 2024173.

The related parameters of crystals, and the data of the bond length and bond angle are summarized in the ESI.† The central iridium is in a hexahedral octahedral configuration, surrounded by C and N atoms of the MPBFP ligand and O atoms of diketone, which is consistent with the reported parameter of metal iridium complexes in literature.[20,21]

3.3 UV-visible absorption and photoluminescence spectra

Fig. 3 shows the UV-vis absorption and fluorescence spectra of the three iridium complexes in the solution. It can be seen from Fig. 3(I) that iridium complexes, $(MPBFP)_2Ir(detd)$, $(MPBFP)_2Ir(tmd)$ and $(MPBFP)_2Ir(acac)$, all show strong absorption in the range of 260–340 nm, attributable to the electronic π–π* transition of MPBFP. Moreover, it is known that the weak absorption around 450–500 nm is a characteristic peak of Ir(III) complexes, meaning the spin allowed singlet transition with a charge transfer character from the metal to the ligand pyridine unit (^{1}MLCT), and slightly allowed the triplet transition from the metal d orbital to the ligand Π* orbital induced by the strong spin–orbit coupling effects of heavy iridium atom (^{3}MLCT).

Fluorescence spectroscopy of the three complexes, namely $(MPBFP)_2Ir(detd)$, $(MPBFP)_2Ir(tmd)$ and $(MPBFP)_2Ir(acac)$, are displaced in Fig. 3(II). The maximum emission wavelengths of $(MPBFP)_2Ir(detd)$, $(MPBFP)_2Ir(tmd)$ and $(MPBFP)_2Ir(acac)$ are 537 nm, 544 nm and 540 nm, respectively, when excited at 260 nm wavelength. The shifts of emission peak may be due to the substituent effects on the diketone ancillary ligand. As mentioned above, the difference of the three ancillary ligands is the alkyl groups on the diketone's backbone: detd has two

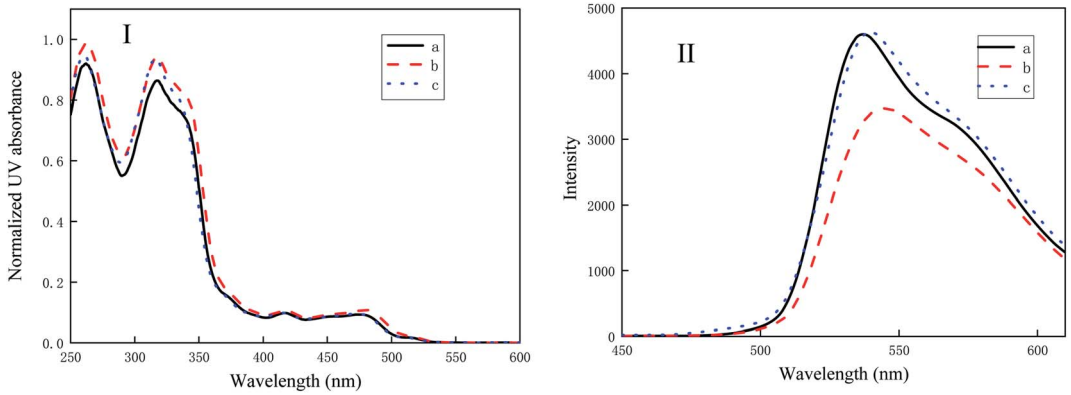

Fig. 3 The absorption spectra (I) and fluorescence spectra (II) of the three complexes: (a) $(MPBFP)_2Ir(detd)$, (b) $(MPBFP)_2Ir(tmd)$, (c) $(MPBFP)_2Ir(acac)$. The measuring conditions are in dichloromethane with a concentration of 1×10^{-5} M, respectively.

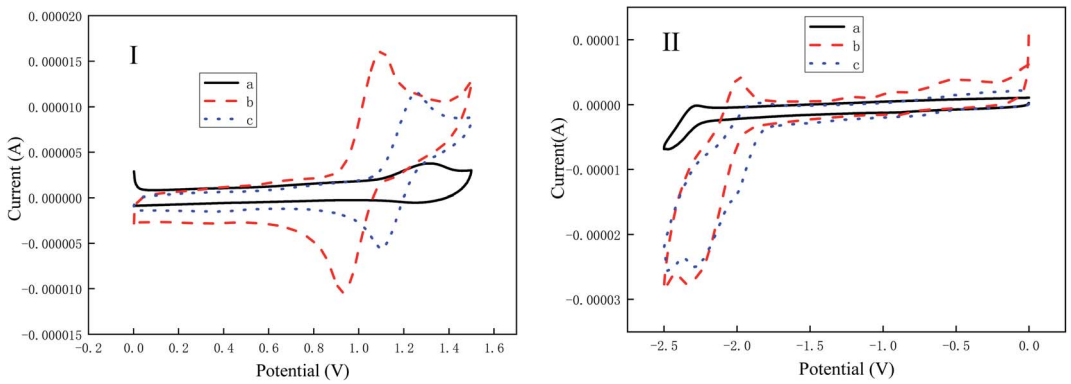

Fig. 4 Oxidation and reduction potential curves of the three iridium complexes. (I) Oxidation potential, (II) reduction potential, (a) $(MPBFP)_2Ir(detd)$, (b) $(MPBFP)_2Ir(tmd)$, (c) $(MPBFP)_2Ir(acac)$. All measurements were performed in methylene chloride solution with ferrocene the Fermi energy of 4.8 eV is the reference.

Table 1 Electrochemical properties of the three iridium complexes: (a) $(MPBFP)_2Ir(detd)$, (b) $(MPBFP)_2Ir(tmd)$, (c) $(MPBFP)_2Ir(acac)$[a]

Samples	E^{red}/V	E^{oxd}/V	E^{Fe}/V	LUMO/eV	E_g/eV	HOMO/eV
a	−1.84	1.28	0.78	−2.18	3.12	−5.30
b	−1.92	1.13	0.68	−2.20	3.05	−5.25
c	−1.80	1.24	0.79	−2.21	3.04	−5.25

[a] E^{red}, reducing potential; E^{oxd}, oxidation potential; LUMO, minimum unoccupied orbital domain; E_g, energy difference between the ground state and the excited state; HOMO, highest occupied orbital domain.

pentyl groups, tmd has two *tert*-butyl groups, while acac has two methyl groups. The three kinds of alkyl groups (R) displace different electronic and steric effects for the diketone ligands and MPBFP ligands. The wavelength shift is the result of the combined effect of these two interactions. This indicates that we can adjust the emission wavelength by changing the substituent groups.

3.4 Electro chemical properties

Fig. 4 shows oxidation and reduction potential curves of the three iridium complexes. The oxidation potentials of $(MPBFP)_2Ir(detd)$, $(MPBFP)_2Ir(tmd)$ and $(MPBFP)_2Ir(acac)$ are 1.28 V, 1.13 V, 1.24 V, respectively. The corresponding reduction potentials of them three are −1.84 V, −1.92 V, and −1.80 V. The oxidation of metallic iridium complexes usually occurs at the metal-center d electron, and the reduction potential is derived from the reduction of pyridine units in phenylpyridine ligands. The results of the oxidation and reduction potential data of the three iridium complexes are summarized in Table 1. For the three iridium complexes, their HOMO and LUMO electron density distributions are similar; however, because of different substituent groups R, their HOMO and LUMO energy levels show some subtle difference, for example, $\Delta_{HOMOmax}$ is 0.05 eV and $\Delta_{LUMOmax}$ is 0.03 eV. Energy difference between the ground state and the excited state is consistent with the spectrum result.

3.5 Electroluminescence performance

To investigate the electroluminescence (EL) properties of the three materials, they were used as dopants to prepare OLED devices. The guest material iridium complexes doped with the host material TCTA with concentrations varying from 10 wt%, 12 wt% to 15 wt%, Bebp2 as the electron transport material, and LiF:Al forming a double cathode.

Fig. 5 shows the electroluminescence spectra of $(MPBFP)_2$-Ir(detd) under various drive voltages at different doping weight percentages dispersed in the organic light-emitting layer of the

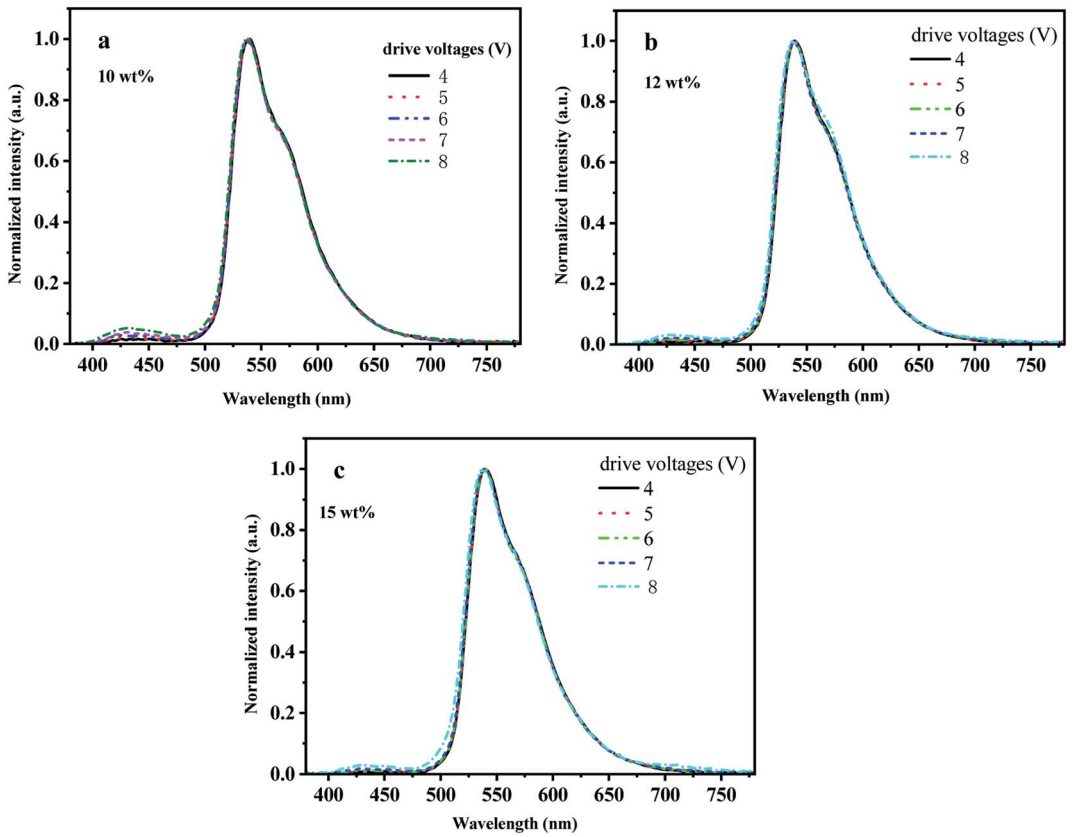

Fig. 5 Electroluminescence spectra of $(MPBFP)_2Ir(detd)$ under various drive voltages at different doping weight percentages dispersed in the organic light-emitting layer of the electroluminescent devices: (a) 10 wt% (b) 12 wt% (c) 15 wt%. The emission peaks are 538 nm, 539 nm and 539 nm, respectively.

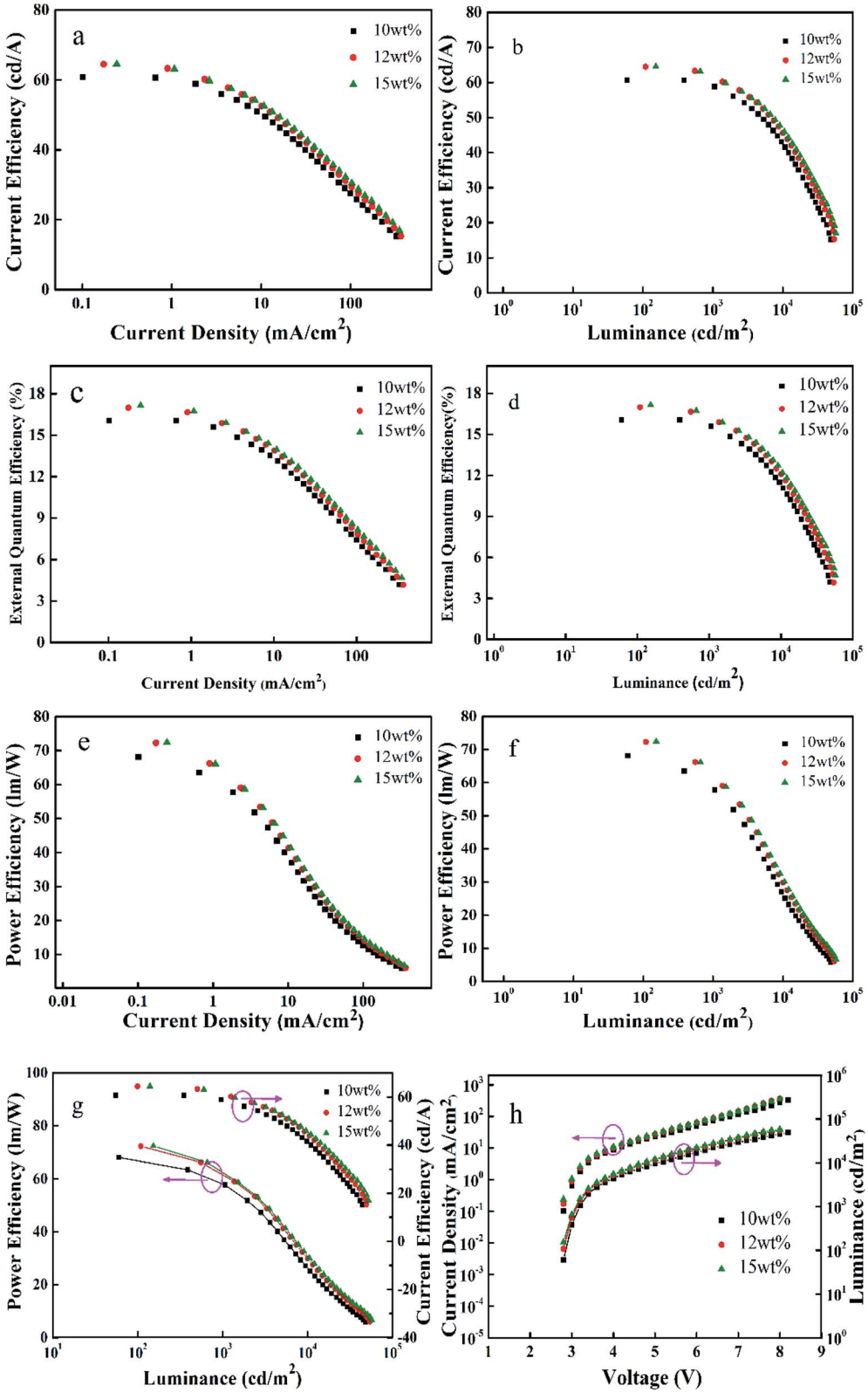

Fig. 6 EL properties of the fabricated OLED devices with $(MPBFP)_2Ir(detd)$ as dopants, (a) current density ~ current efficiency curve, (b) brightness ~ current efficiency curve, (c) current density ~ external quantum efficiency curve, (d) brightness ~ external quantum efficiency curve, (e) current density ~ power efficiency curve, (f) brightness ~ power efficiency curve, (g) brightness ~ power efficiency ~ current efficiency curve, (h) voltage ~ current density ~ brightness curve.

Table 2 Electroluminescence performance of the fabricated OLED devices with dopants of $(MPBFP)_2Ir(detd)$, $(MPBFP)_2Ir(tmd)$, $(MPBFP)_2Ir(acac)$

Dopant	Doping concentration (wt%)	Bri max[f] ($mA\ cm^{-2}$)	EQE[a] max/%	CE[b] max ($cd\ A^{-1}$)	PE[c] max ($lm\ W^{-1}$)	CIE[d] (x, y)[e]	Peak max/nm
$(MPBFP)_2Ir(detd)$	10	48 470 @ 8 V	16.1 @ 2.8 V	60.7 @ 2.8 V	68.1 @ 2.8 V	(0.39, 0.58)	538
	12	54 505 @ 8 V	17.0 @ 2.8 V	64.4 @ 2.8 V	72.3 @ 2.8 V	(0.39, 0.58)	539
	15	57 328 @ 8 V	17.2 @ 2.8 V	64.5 @ 2.8 V	72.4 @ 2.8 V	(0.39, 0.58)	539
$(MPBFP)_2Ir(tmd)$	10	63 863 @ 8 V	15.7 @ 2.8 V	58.9 @ 2.8 V	66.0 @ 2.8 V	(0.40, 0.58)	544
	12	70 965 @ 8 V	16.3 @ 2.8 V	61.3 @ 2.8 V	68.7 @ 2.8 V	(0.40, 0.57)	544
	15	69 267 @ 8 V	16.7 @ 2.8 V	62.2 @ 2.8 V	69.8 @ 2.8 V	(0.40, 0.57)	545
$(MPBFP)_2Ir(acac)$	10	55 287 @ 7.5 V	15.5 @ 3.1 V	58.9 @ 3.1 V	66.0 @ 3.1 V	(0.38, 0.57)	540
	12	52 179 @ 7.5 V	16.3 @ 3.0 V	60.7 @ 3.0 V	66.6 @ 3.0 V	(0.38, 0.56)	539
	15	55 750 @ 7.5 V	16.5 @ 3.0 V	61.7 @ 3.0 V	64.6 @ 3.0 V	(0.40, 0.57)	541

[a] Maximum external quantum efficiency. [b] Maximum current efficiency. [c] Power efficiency. [d] Commission Internationale de l'Eclairage. [e] The CIE values are measured at 5 V. [f] The number after @ indicates the corresponding voltage value.

electroluminescent devices. The devices emit green light with an EL spectrum peak at 537 nm. It should also be noted that there is a weak signal between 400 and 450 nm on the EL spectra for all devices, and they were attributed to the emission of the host material TCTA residue, which is the result of inefficient energy transfer from the host material to the dopant materials. By increasing the dopant concentration from 10% to 15%, the emission from the host materials decreased (Fig. 6).

Fig. 6 illustrates the EL properties of the fabricated OLED devices with $(MPBFP)_2Ir(detd)$ as dopants. EL performance of the devices prepared with $(MPBFP)_2Ir(detd)$, $(MPBFP)_2Ir(tmd)$ and $(MPBFP)_2Ir(acac)$ at doping concentrations of 10%, 12% and 15% are summarized in Table 2, where the CIE was measured under a voltage of 5 V. From the data mentioned above, we can draw a few conclusions: for example, doping concentration has no effect on CIE values, 15 wt% is an appropriate ratio among the three, and $(MPBFP)_2Ir(detd)$ performs better than the other two iridium complexes. The 15 wt% $(MPBFP)_2Ir(detd)$ device performed the highest value for external quantum efficiency of 17.2%, with current efficiency of 64.5 $cd\ A^{-1}$ and power efficiency of 72.4 $lm\ W^{-1}$. This result can be explained by the substituent effects on the β-diketone ancillary ligand. The detd has two pentyl groups, which can effectively reduce the interchain interaction between the dye molecules in the process of evaporation, and thus reduce the aggregation quenching effects for the OLED devices.

4. Conclusions

We have designed and synthesized a new main ligand MPBFP, and then complexed it with three β-diketone auxiliary ligands to obtain three new metal iridium complexes, namely $(MPBFP)_2Ir(detd)$, $(MPBFP)_2Ir(tmd)$ and $(MPBFP)_2Ir(acac)$. The three metal complexes of iridium are soluble in organic solvents and suitable for the solution method to prepare OLED devices. Studies on thermal stability, photophysical properties and electrochemical properties show that the modification of the substituent groups on the auxiliary ligand can change HOMO and LUMO energy levels and emission wavelengths.

Author contributions

Zequn Ma, investigation, writing – original draft, Chaojun Jing, conceptualization, writing – review & editing, Deyu Hang, funding acquisition, project administration, Hongtao Fan, formal analysis, Lumeng Duan, resources, supervision, Shuqing Fang, investigation, data curation, Li Yan, resources.

Conflicts of interest

There are no conflicts to declare.

Acknowledgements

Electroluminescence performance testing of the complexes was performed by State Key Laboratory of Luminescent Materials and Devices, South China University of Technology.

Notes and references

1 J. Y. Shao, J. Yao and Y. W. Zhong, Mononuclear cyclometalated ruthenium(II) complexes of 1,2,4,5-tetrakis (*N*-methylbenzimidazolyl) benzene: synthesis and electrochemical and spectroscopic studies, *Organometallics*, 2012, **31**(11), 4302–4308.

2 B. Umamahesh, N. S. Karthikeyan, K. I. Sathiyanarayanan, *et al.*, Tetrazole iridium(III) complexes as a class of phosphorescent emitters for high-efficiency OLEDs, *J. Mater. Chem. C*, 2016, **4**(42), 10053–10060.

3 B. Ma, E. Barron, A. DeAngelis, *et al.*, Metal complex for phosphorescent OLED, *US Pat.*, 10,355,227[P], 2019-7-16.

4 P. K. Samanta, D. Kim, V. Coropceanu, *et al.*, Up-conversion intersystem crossing rates in organic emitters for thermally activated delayed fluorescence: impact of the nature of singlet *vs.* triplet excited states, *J. Am. Chem. Soc.*, 2017, **139**(11), 4042–4051.

5 H. Sun, C. Zhong and J. L. Bredas, Reliable prediction with tuned range-separated functionals of the singlet–triplet gap in organic emitters for thermally activated delayed

fluorescence, *J. Chem. Theory Comput.*, 2015, **11**(8), 3851–3858.

6 H. Kaji, H. Suzuki, T. Fukushima, *et al.*, Purely organic electroluminescent material realizing 100% conversion from electricity to light, *Nat. Commun.*, 2015, **6**, 8476.

7 E. C. Smith, F. Qureshi and J. Jongman, Organic electroluminescent device, *US Pat.*, 9,136,504[P], 2015-9-15.

8 M. Kim, S. K. Jeon, S. H. Hwang, *et al.*, Stable Blue Thermally Activated Delayed Fluorescent Organic Light-Emitting Diodes with Three Times Longer Lifetime than Phosphorescent Organic Light-Emitting Diodes, *Adv. Mater.*, 2015, **27**(15), 2515–2520.

9 Z. Ren, R. S. Nobuyasu, F. B. Dias, *et al.*, Pendant Homopoly and Copolymers as Solution-Processable Thermally Activated Delayed Fluorescence Materials for Organic Light-Emitting Diodes, *Macromolecules*, 2016, **49**(15), 5452–5460.

10 K. Yoshida, H. Nakanotani and C. Adachi, Effect of Joule heating on transient current and electroluminescence in pin organic light-emitting diodes under pulsed voltage operation, *Org. Electron.*, 2016, **31**, 287–294.

11 Z. H. Kafafi. *Organic electroluminescence[M]*. CRC Press, 2018.

12 J. H. Seo, Y. K. Kim and Y. Ha, Efficient blue-green organic light-emitting diodes based on heteroleptic tris-cyclometalated iridium (III) complexes, *Thin Solid Films*, 2009, **517**(5), 1807–1810.

13 A. Ito, T. Hiokawa, E. Sakuda, *et al.*, Bright Green-phosphorescence from Metal-to-boron Charge-transfer Excited State of a Novel Cyclometalated Iridium(III) Complex, *Chem. Lett.*, 2010, **40**(1), 34–36.

14 M. Lepeltier, F. Morlet-Savary, B. Graff, *et al.*, Efficient blue green organic light-emitting devices based on a monofluorinated heteroleptic iridium(III) complex, *Synth. Met.*, 2015, **199**, 139–146.

15 L. Xiao, Z. Chen, B. Qu, *et al.*, Recent progresses on materials for electrophosphorescent organic light-emitting devices, *Adv. Mater.*, 2011, **23**, 926–952.

16 X. Zhang, D. Jacqueemin, Q. Peng, *et al.*, General approach to compute phosphorescent OLED efficiency, *J. Phys. Chem. C*, 2018, **122**(11), 6340–6347.

17 B. N. Yang and D. M. Shin, The Synthesis and Properties of Solution Processable a Red Phosphorescent Iridium(III) Complex with Alkyl Group, *J. Nanosci. Nanotechnol.*, 2016, **16**(3), 2696–2700.

18 H. J. Zeng, M. J. Lin, *et al.*, White Phosphorescent Star-Shape Polymers Derived from Poly (fluorene-carbazole) with Green-Yellow Iridium Complex as the Cores, *Chin. J. Appl. Chem.*, 2020, **1**(39), 17–23.

19 S. Q. Fang, J. S. Qian, D. Y. Hang, *et al.*, Synthesis, characterization and photoelectric properties of β-diketone ruthenium complexes, *Fine Chemicals*, 2020, **4**(37), 786–792.

20 G. Y. Ding, W. L. Jiang, X. Chang, *et al.*, Properties of Yellow-Green Organic Light-Emitting Devices Based on (*E*)2-(2-(9-ethyl-9*H*-carbazol-3-yl)vinyl) Quinolato-Zinc, *Acta Phys.-Chim. Sin.*, 2009, **25**(5), 958–962.

21 F. So, J. Kido and P. Burrows, Organic light-emitting devices for solid-state lighting, *MRS Bull.*, 2008, **33**(7), 663–669.